Timing properties and pulse shape discrimination of LAB-based liquid scintillator*

LI Xiao-Bo(李小波)[1,4;1)] XIAO Hua-Lin(肖华林)[2] CAO Jun(曹俊)[1]
LI Jin(李金)[1] RUAN Xi-Chao(阮锡超)[3] HENG Yue-Kun(衡月昆)[1]

[1] Experimental Center, Institute of High Energy Physics, Chinese Academy of Sciences, Beijing 100049, China
[2] College of Nuclear Science and Technology, Beijing Normal University, Beijing 100875, China
[3] China Institute of Atomic Energy, Beijing 102413, China
[4] Graduate University of Chinese Academy of Sciences, Beijing 100049, China

Abstract: Linear Alkyl Benzene (LAB) is a promising liquid scintillator solvent in neutrino experiments because it has many appealing properties. The timing properties of LAB-based liquid scintillator have been studied through ultraviolet and ionization excitation in this study. The decay time of LAB, PPO and bis-MSB is found to be 48.6 ns, 1.55 ns and 1.5 ns, respectively. A model can describe the absorption and re-emission process between PPO and bis-MSB perfectly. The energy transfer time between LAB and PPO with different concentrations can be obtained via another model. We also show that the LAB-based liquid scintillator has good (n, γ) and (α, γ) discrimination power.

Key words: linear alkyl benzene, decay time, pulse shape discrimination, energy transfer time

PACS: 29.40.Mc **DOI:** 10.1088/1674-1137/35/11/009

1 Introduction

Large volume organic liquid scintillators have made great contributions to low energy neutrino physics for rare event detection [1–3]. In this paper, we will study the timing properties of the liquid scintillator with LAB as a solvent, PPO as a primary fluorescence material, and bis-MSB as wavelength shifter, which has been adopted in the Daya Bay reactor neutrino experiment [2]. When charged particles interact with the liquid scintillator, most ionization and excitation happen on the solvent molecules due to their large quantities with respect to the solutes. In general, solvents have a rather low efficiency in converting their excitation energy to scintillation light. Solutes are added to improve this efficiency. Sometimes a wavelength shifter is added to match the emission spectrum of the mixtures to the sensitivity curve of photomultipliers (PMT).

As a new type of liquid scintillator solvent, LAB has many attractive characteristics, such as a high flash point, its low cost, its chemical compatibility with acrylic (which has a lower radioactivity than glass vessels), its long stability and good transparency [4–7]. It is also the preferred solvent candidate of next generation experiments like SNO+ and LENA (Low Energy Neutrino Astronomy) [8]. The timing properties of LAB-based liquid scintillator are studied in this paper.

A classical single photon method is widely used in fluorescence decay time measurements [9–13]. Fast and slow time constants of fluorescence can be derived from the fit of the time profile of the liquid scintillator. Only the fast component has an intrinsic meaning [12, 14]. The slow component is complicated and cannot be easily described as a simple power law like the fast component. Therefore, the decay time constant referred to in this paper only applies to the fast component. The intrinsic decay time of solvent and solutes is measured because it is relevant to light propagation. If a fluorescent photon is absorbed in the scintillator, the probability of re-emission and its timing characteristics are determined by the quantum efficiency and

Received 12 February 2011, Revised 7 April 2011
* Supported by National Natural Science Foundation of China (10890094, 11011120080)
1) E-mail: lixb@ihep.ac.cn

intrinsic decay time of the absorbing molecules. A model proposed in this study can well describe this process.

2 The timing properties of LAB-based liquid scintillator

2.1 Experimental setup

The experimental setup for the time response of the liquid scintillator (LS) to ultraviolet laser excitation is shown schematically in Fig. 1. When the pulsed diode laser emits, a synchronous pulse is also output.

The emission spectrum of the laser was measured by a QE65000 Scientific-grade Spectrometer from Ocean Optics, shown in Fig. 1. The peak value of the emission is about 282 nm with a width of about 10 nm. The photons go through an optical fiber and a quartz vessel (1 cm×1 cm×3 cm) filled with liquid samples. Molecules in the LS will be excited and then scintillation light will emit isotropically. The laser intensity and the distance between the vessel and the PMT are tuned to guarantee that the probability of detecting a single photoelectron (PE) of a scintillation event is less than 9%, thus the contribution from multiple PEs can be ignored in the analysis. The signals from the synchronous output of the laser and the PMT (XP2020) are fed to the start and stop inputs of TDC (CEAN C414) after they go through the Constant Fraction Discriminators (CFD) respectively. In order to convert the TDC channels to time, the ORTEC 462 Time Calibrator with a range of 320 ns and a period of 10 ns was adopted to calibrate the TDC before our measurements. The results are shown in Fig. 2.

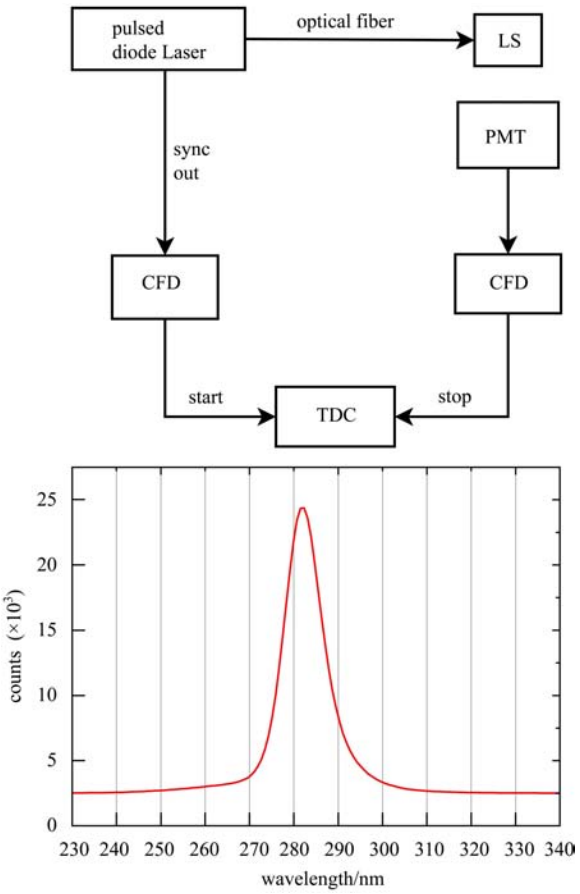

Fig. 1. Single photon method under ultraviolet excitation. Top: Schematic view of the experimental setup. Bottom: The emission spectrum of pulsed diode laser.

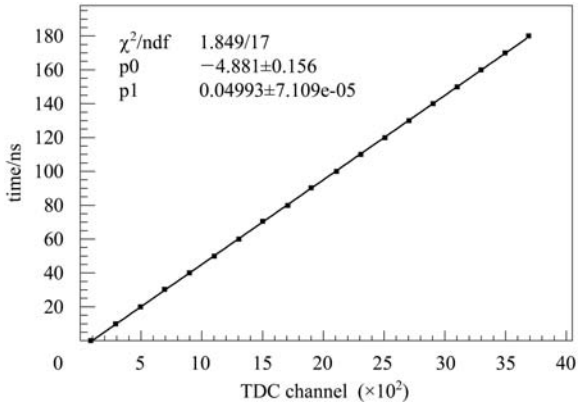

Fig. 2. The TDC calibration result (49.9 ps/channel).

The intrinsic time response of the instrumentation can be obtained by removing the LS vessel from the setup in Fig. 1 and placing the PMT in front of the laser. The time response is shown in Fig. 3. The full width at half maximum (FWHM) is about 750 ps,

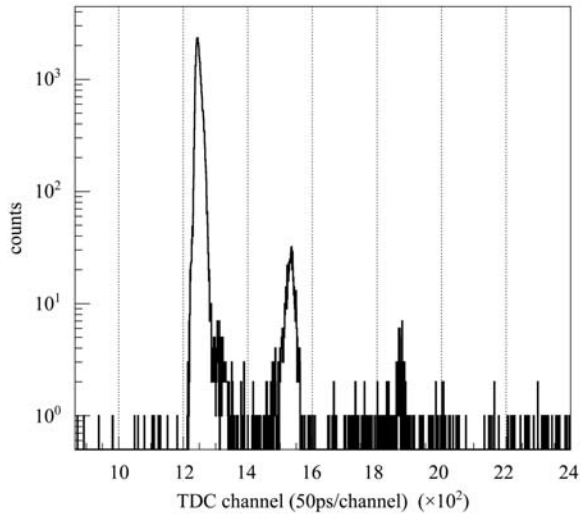

Fig. 3. The time response of the instrumentation (FWHM=750 ps). The small peaks at about 1550 channels and 1900 channels are due to fast after-pulses of the PMT.

mainly caused by the time jitter of the laser and the PMT. Small peaks appearing at about 1550 channels and 1900 channels are caused by the fast after-pulses of the PMT. It is verified by the fact that they will shift leftward when the voltage of the PMT is tuned higher.

2.2 Decay time and oxygen quenching of LAB-based LS

Two samples of LAB are added to the vessel in Fig. 1 separately. One is thoroughly bubbled with nitrogen to eliminate oxygen dissolved in the liquid and the other one is not bubbled. Their light-pulse shapes are displayed in Fig. 4. The probability density function of the scintillation time can be described by a convolution of the scintillator decay time with the instrumental response, which is often taken as Gaussian [10, 15], as shown in Eq. (1). Dispersion σ and mean time delay T are described to characterize the Gaussian function of the instrumental response. However, the time response of our instrument is not a Gaussian distribution and also has the effect of an after pulse. The measured time response shown in Fig. 3 is used to replace the Gaussian distribution as shown in Eq. (2).

$$I(t)=\int_0^t \frac{C}{\sqrt{2\pi}\sigma}\mathrm{e}^{-\frac{(t-T-t')^2}{2\sigma^2}}\left(\frac{\omega}{\tau_0}\mathrm{e}^{-\frac{t'}{\tau_0}}+\frac{1-\omega}{\tau_1}\mathrm{e}^{-\frac{t'}{\tau_1}}\right)\mathrm{d}t', \tag{1}$$

$$I(t)=C\int_0^t R(t-t')\left(\frac{\omega}{\tau_0}\mathrm{e}^{-\frac{t'}{\tau_0}}+\frac{1-\omega}{\tau_1}\mathrm{e}^{-\frac{t'}{\tau_1}}\right)\mathrm{d}t', \tag{2}$$

where C is the coefficient representing the statistics of the measurement. *R(t)* is the function of instrumental response. τ_0 and τ_1 are the decay times of the fast and slow components of the scintillation light, and ω describes the fraction of the fast component. The fitted decay time of the bubbled LAB is about 48.6 ns as shown in Fig. 4. For the unbubbled LAB sample, the decay time is around 30 ns. The long lifetime of the excited LAB molecules allows oxygen molecules enough time to interact with the excited LAB molecules and quench them, causing them to return to the ground state without emitting fluorescence.

Three liquid scintillator samples, LAB+3 g/L PPO with and without bubbling, and LAB+15 g/L PPO without bubbling, are measured under the same conditions as above. The results are shown in Fig. 5. There is almost no difference in time response between these three samples. Thus we can conclude that a) when excited by UV light, there is no energy transfer between the LAB and PPO molecules. The

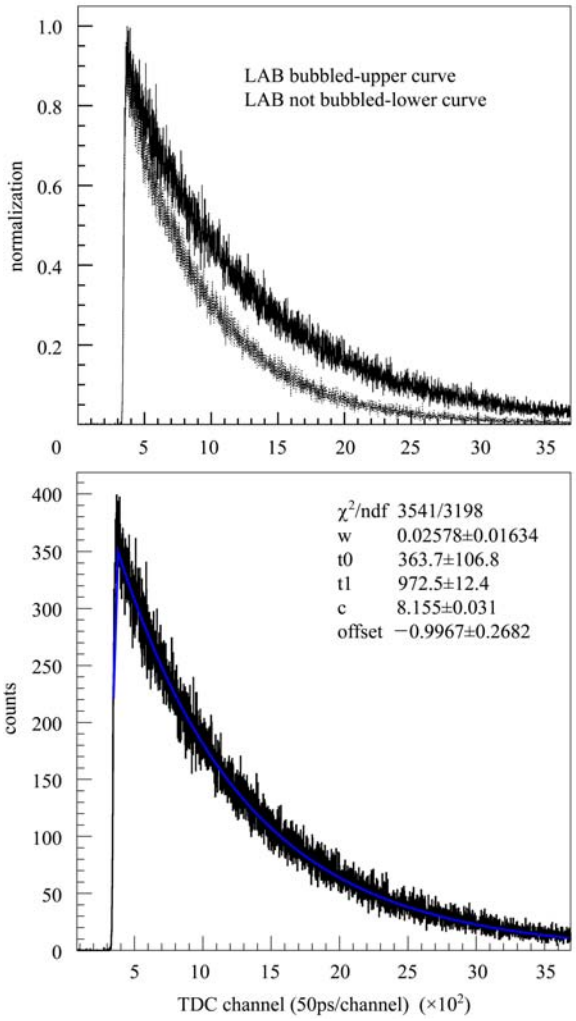

Fig. 4. LAB under ultraviolet excitation. Top: The effect of oxygen quenching on decay time of LAB. Bottom: The decay time of LAB bubbled with nitrogen (τ_0=48.6 ns).

scintillation light is from PPO directly excited by UV light. Otherwise we should be able to see the quenching effect from LAB by comparing the samples with and without bubbling. It further indicates that the absorption of UV light at 270–300 nm in these samples is dominated by PPO, when its concentration is large. b) The short decay time of PPO offers little chance for oxygen to interact with the excited molecules. From other studies [16], we know that oxygen will quench the scintillation light when excited by ionization, because the directly excited molecules are LAB. Using UV excitation, we can get the intrinsic decay time of PPO from the above measurements. It is about 1.55 ns as shown in Fig 5. We used the measured time response of the instrumentation in the fitting. If using Gaussian, the fitted decay time is about 1.69 ns.

Cyclohexane is almost transparent to photons at about 280 nm. A similar measurement is done by dissolving bis-MSB in cyclohexane. The decay time of bis-MSB is shown in Fig. 6. The intrinsic decay time of bis-MSB is found to be 1.5 ns. Again, oxygen quenching cannot affect it due to its short decay time.

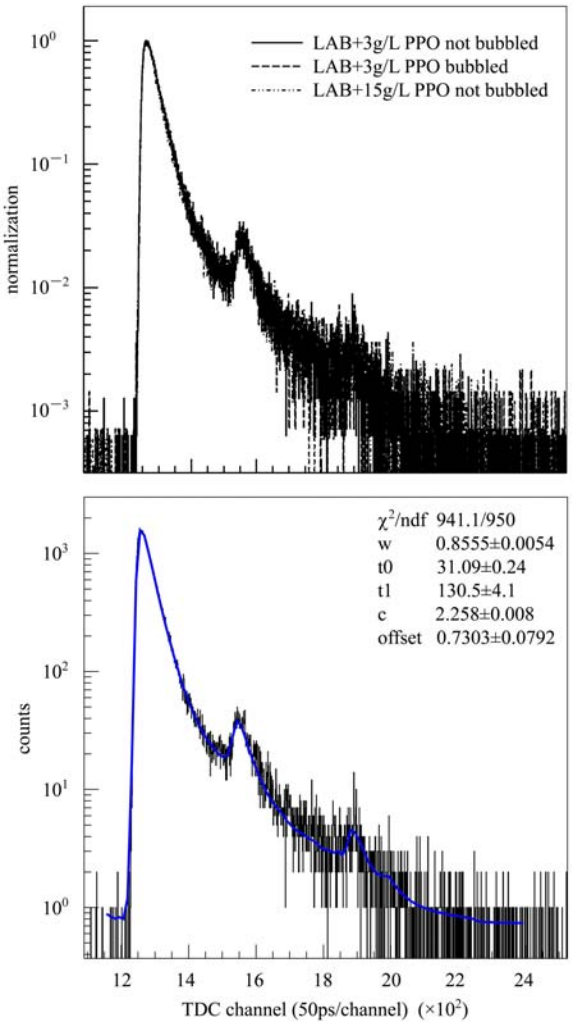

Fig. 5. Top: Decay time of LAB+PPO system under ultraviolet excitation. Bottom: Intrinsic decay time fitting of PPO (τ_0=1.55 ns).

As for a ternary system LAB+3 g/L PPO+15 mg/L bis-MSB, laser photons will be absorbed by PPO first, because the absorption by LAB and bis-MSB is negligible at ∼280 nm compared to PPO in this LS. Fluorescence photons will be emitted from the excited states of PPO. Some of them will be absorbed and re-emitted by bis-MSB. The attenuation lengths of 3 g/L PPO and 15 mg/L bis-MSB were also measured in Ref. [17]. Now the timing of photons detected by the PMT is determined by many factors, such as the absorption-reemission fraction of photons, the vessel size and the quantum efficiency curve of the photocathode, among others. Suppose the intrinsic decay time of bis-MSB can be approximated as a single exponential of time constant τ_3. The ω fraction of detected light is due to the absorption and reemission of bis-MSB and the $1-\omega$ fraction is from PPO directly. The time response of the ternary LS can be described as Eq. (3)

$$I(t'') = C\int_0^{t''}\left[\int_0^t \omega\left(\frac{\omega_1}{\tau_1}\mathrm{e}^{-\frac{t'}{\tau_1}}+\frac{1-\omega_1}{\tau_2}\mathrm{e}^{-\frac{t'}{\tau_2}}\right)\times\frac{1}{\tau_3}\mathrm{e}^{-\frac{t-t'}{\tau_3}}\mathrm{d}t'+(1-\omega)\left(\frac{\omega_1}{\tau_1}\mathrm{e}^{-\frac{t}{\tau_1}}+\frac{1-\omega_1}{\tau_2}\mathrm{e}^{-\frac{t}{\tau_2}}\right)\right]R(t''-t)\mathrm{d}t, \quad (3)$$

where $(\omega_1,\ \tau_1)$ and $(1-\omega_1,\ \tau_2)$ describe the fraction and time constant of the fast and slow components of PPO, respectively. R(t) is again the measured instrumental response. The fit result is shown in Fig. 6.

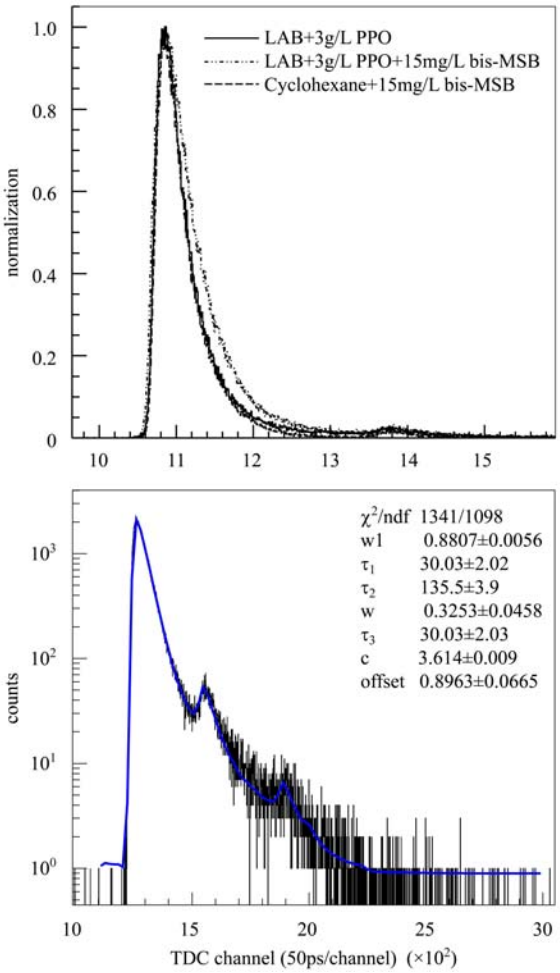

Fig. 6. Top: Decay time curve of a bis-MSB system under ultraviolet excitation. Bottom: Decay time fit of the LS (LAB +3 g/L PPO+ 15 mg/L bis-MSB) under ultraviolet excitation.

The decay time of the LS is well described by the above model. The fitted time constants of PPO and bis-MSB are both 1.5 ns, which are consistent with the individual measurements. The re-emission fraction ω for our experimental setup is 32%.

2.3 Energy transfer time from LAB to PPO

In order to study the energy transfer process from LAB to PPO, ionizing particles are exploited to excite the liquid samples. Unlike UV light which excites the PPO directly due to its large optical absorption, the ionizing particles will excite the LAB molecules due to their large quantity compared with the solutes. A fast PMT, closely coupled to the vessel in Fig. 1, replaces the laser to supply as the start input of TDC. This PMT can detect a burst of photons when ionizing particles deposit energy in liquid samples. Statistically it will provide the start time of the scintillation event. A ^{60}Co γ source is located in front of the vessel. In the LAB+PPO system, scattered electrons ionize and excite LAB molecules which will transfer their energy to PPO mostly via a non-radiative mechanism. The observed fluorescence photons come from the radiative decay of PPO molecules.

Four samples with different concentrations of PPO in LAB with no nitrogen bubbling have been prepared. Their decay curves have been measured with ^{60}Co radiation as shown in Fig. 7. Eq. (4) can be used to describe the time response of the γ radiation.

$$I(x) = C\int_0^x \left[\int_0^t \left(\frac{\omega_1}{\tau_1}\mathrm{e}^{-\frac{t'}{\tau_1}} + \frac{1-\omega_1}{\tau_2}\mathrm{e}^{-\frac{t'}{\tau_2}}\right) \times \frac{1}{\tau_3}\mathrm{e}^{-\frac{t-t'}{\tau_3}}\mathrm{d}t'\right] R(x-t)\mathrm{d}t. \quad (4)$$

where (ω_1, τ_1) and ($1-\omega_1$, τ_2) represent the fraction and time constant of the fast and slow components of the energy transfer time from LAB to PPO, respectively. τ_3 is the intrinsic time of PPO. The fast energy transfer time (τ_1), its weight (ω_1) and intrinsic time of PPO (τ_3) are shown in Table 1 when PPO has different concentrations in LAB.

Table 1. The fast energy transfer time from LAB to PPO, its weight and intrinsic time of PPO.

sample	τ_1/ns	ω_1	τ_3/ns
LAB+1g/L PPO	4.18	49.3%	1.6
LAB+3g/L PPO	3.1	71.4%	1.33
LAB+5g/L PPO	2.33	76.2%	1.42
LAB+7g/L PPO	2.08	77.6%	1.3

The energy transfer time becomes smaller when PPO concentration increases. It means that the energy transfer time from LAB to PPO decreases when PPO concentration increases, since the collision probability of LAB and PPO molecules increases. Once the PPO concentration reaches a certain level, additional PPO only decreases the energy transfer time slightly. Although PPO is as high as 7 g/L in the measurements, the time profile cannot reach the same as the PPO intrinsic time response.

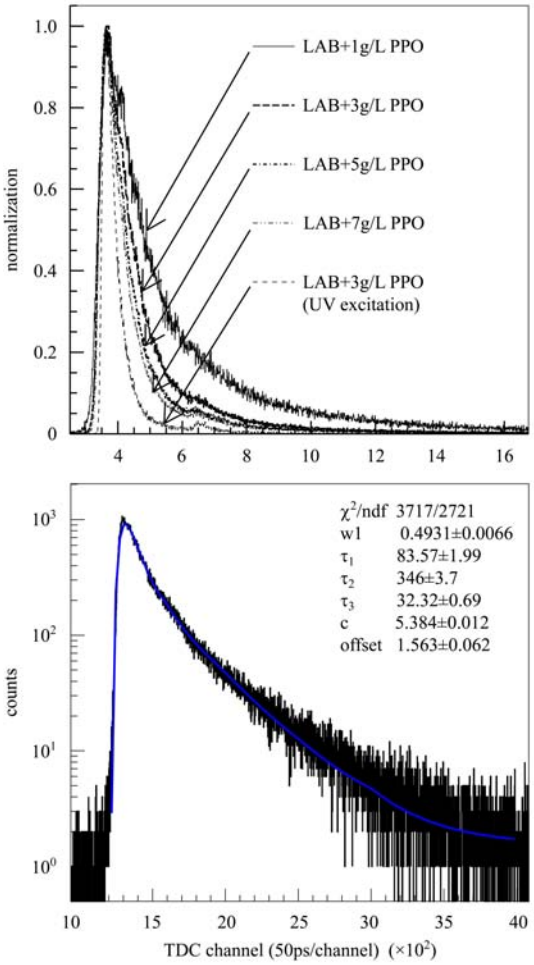

Fig. 7. Top: The decay time curves of different concentrations of PPO in LAB under γ radiation. Bottom: The decay time fit of LS (LAB+1 g/L PPO) under ^{60}Co radiation.

3 Pulse shape discrimination of the LAB-based liquid scintillator

3.1 (n, γ) discrimination

The time response of the ternary LS, LAB+3 g/L PPO+15 mg/L bis-MSB, to fast neutrons was measured at the China Institute of Atom Energy (CIAE), using the Pulsed Neutron Generator. The pulsed neutrons were generated by the D(T,n)α reaction with a 250 keV deuteron beam impinging on a T-Ti target.

The frequency of the pulse is 1.5 MHz, with a pulse width of about 2 ns. The detector is located at a distance of 3.7 meters from the target and 45 degrees with respect to the direction of the deuterium beam. The neutron energy is mono-energetic and it is about 14 MeV. The distance was chosen to optimize the event rate. Since neutron radiation was always accompanied with γs, the detector was in the γ and neutron mixing field. The experimental arrangement is shown in Fig. 8. A time of flight (TOF) technique was adopted to distinguish γ and the neutrons.

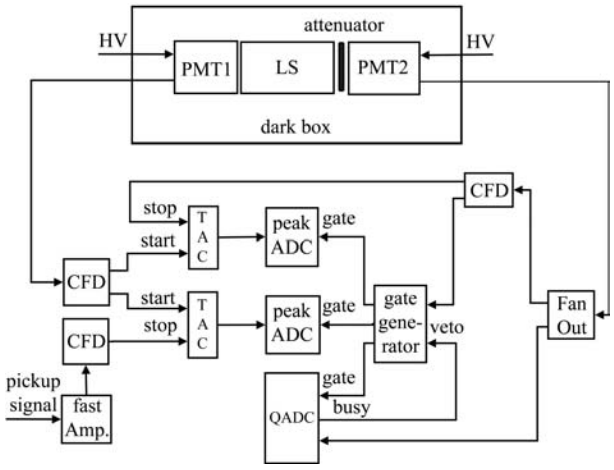

Fig. 8. The experimental setup for neutron irradiation.

The samples are filled in a cylindrical container (5 cm in diameter and 4 cm in height). The anode signal of PMT1 is discriminated by a CFD and divided into two branches. One is used as the start input of a TAC (Time Amplitude Converter) together with the stop input from the delayed pickup signal of the pulsed neutron. This reverse configuration has been adopted to avoid the high rate of start signals not followed by any stop that would occur in the normal setup. The output of the TAC is fed to the peak sensing ADC, and the TOF information can be obtained. The TOF spectrum of the neutron and γ is shown in Fig. 9. The first high peak in the TOF spectrum is the neutrons, while the second small peak near 2200 channels is γ. The other branch is also used as the start input of another TAC while the stop input is from PMT2 after its anode signal goes through CFD. The decay time of the LS will be obtained from the time difference of the γ excitation measurements. The charge of the PMT2 anode signal is derived from the QADC in order to select single photoelectron events which are shown in Fig. 9. The TOF information, the decay time of the LS, and the charge information of PMT2 are recorded simultaneously as an event. A gate generator was used for the gate input of the ADC and supplied 18 μs veto time from QADC in order to avoid new events influencing the ADC conversion when it is under digitalization. The three parameters were saved in list mode. The Kmax CAMAC DAQ system developed by the SPARROW corporation was used. The TAC-ADC calibration result for decay time measurement is 49.7 ps per channel.

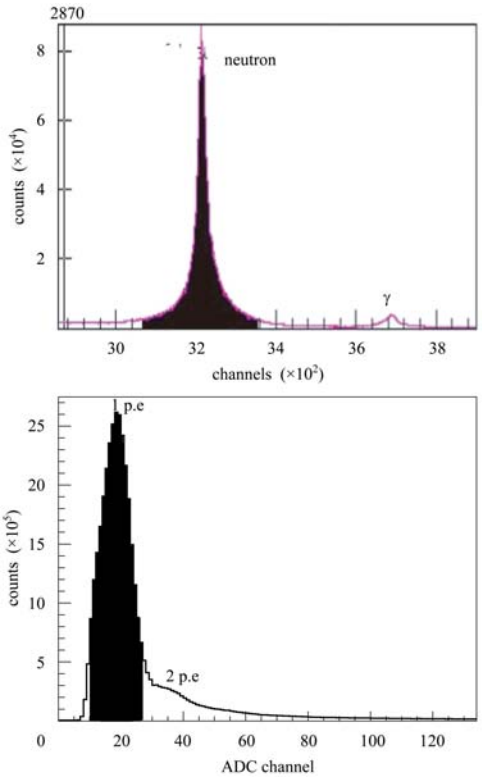

Fig. 9. Top: The TOF spectrum of the neutron and γ. The first peak is the neutron while the small peak near 3700 channels is γ. Bottom: The charge distribution of the anode signal from PMT2 for a single photoelectron selection.

Neutrons will collide with nuclei in the LS. The recoil nuclei will excite the LS molecules. Among the LS nuclei, Hydrogen has the largest cross section compared with other nuclei. Therefore, most of the scintillation is from the ionization and excitation of recoil protons. The scintillation time profiles of the fast neutron and γ are both displayed in Fig. 10. The time profile of γ is also derived by ^{60}Co radiation. The samples were also nitrogen bubbled before measurements were taken. Their slow components are very different. By comparing the fraction of slow light, we could distinguish neutron and γ. The discrimination power depends on the incident particle energy due to the statistics of photons, as well as the vessel size, since the fraction of absorption-reemission light and Rayleigh scattering [18] will be different.

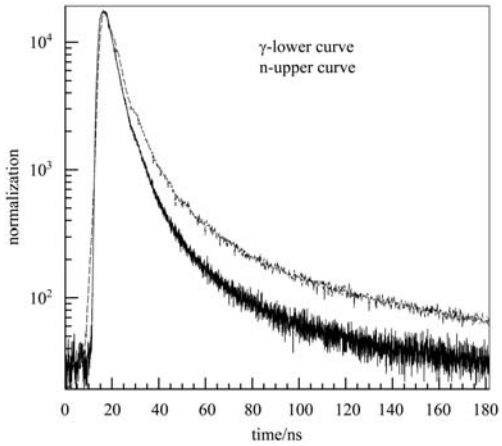

Fig. 10. Scintillation time profile of the LS (LAB+3 g/L PPO+15 mg/L bis-MSB) under γ and fast neutron radiation.

3.2 (α, γ) discrimination

A similar study is performed for α and γ. A ^{60}Co source and a ^{239}Pu source emitting 5.15 MeV α are used. The LS samples are thoroughly bubbled with nitrogen. The results are shown in Fig. 11. As the neutron case, the slow component of α is different from that of γ, which can be used to distinguish these two particles. Again, the discrimination power will depend on the particle energy and the detector size. Detailed simulations or experimental tests need to be done for a given detector setup.

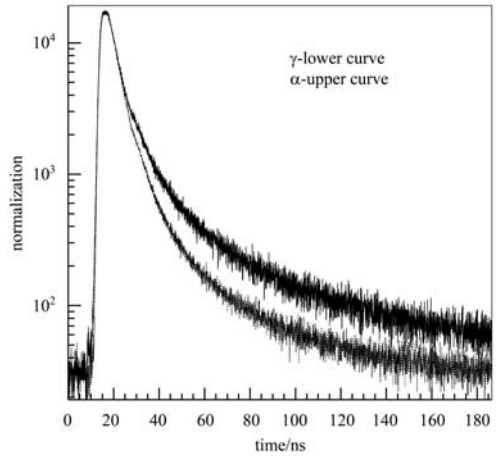

Fig. 11. Scintillation time profile of the LS (LAB+3 g/L PPO+15 mg/L bis-MSB) under γ and α excitation.

4 Conclusions and discussions

The measurements described in this study, based on ultraviolet light and ionizing excitation of solvent and solutes, allow a series of scintillator mixtures to be analyzed and compared. We find that the measured instrumental response instead of a Gaussian distribution can give more accurate scintillation decay times of solvent and solutes. We provide a model to describe the absorption and re-emission process between PPO and bis-MSB. The energy transfer time between LAB and PPO can be extracted from a single photon method. They both show that the intrinsic time of PPO or the lifetime of PPO in the first excited states is about 1.5 ns. The lifetime of LAB (48 ns) is larger than that of another well-known solvent pseudocumene (PC) (27 ns) [18]. The energy transfer time from LAB to PPO is also slightly larger than that from PC to PPO. The timing measurements describe well the energy transfer processes in the liquid scintillator. We also show that the LAB-based liquid scintillator has pulse shape discrimination power.

The authors would like to thank Ya-Yun Ding for supplying all the liquid samples, and Zhi-Jia Sun, Ming Xu, and Song-Lin Wang for their discussions and help on the measurements.

References

1 Eguchi K et al. (KamLAND collaboration). Phys. Rev. Lett., 2003, **90**(2): 021802
2 Daya Bay Proposal, arXiv:hep-ex/0701029
3 Alimonti G et al. Astropart. Phys, 2002, **16**(3): 205
4 CHEN M. Talk at the 3rd International Conference on Flavor Physics, Chung-Li, Taiwan, China, 2005
5 Yeh M et al. Nucl. Instrum, Methods A, 2007, **578**(1): 329–339
6 DING Y et al. Nucl. Instrum. Methods A, 2008, **584**(1): 238–243
7 HUANG P et al. JINST, 2010, **5**: 08007
8 Wurm M et al. Rev. Sci. Instr, 2010, **81**(5): 053301
9 Bollinger L M, Thomas G E. Rev. Sci. Instr, 1961, **32**(9): 1044
10 ZHONG W L et al. Nucl. Instrum. Methods A, 2008, **587**: 300–303
11 Ranucci G et al. Nucl. Instrum. Methods A, 1994, **350**: 338–350
12 Ranucci G, Goretti A, Lombardi P. Nucl. Instrum. Methods A, 1998, **412**: 374–386
13 Undagoitia T M et al. Rev. Sci. Instrum, 2009, **80**(4): 043301
14 Birks J B. The Theory and Practice of Scintillation Counting. Oxford: Pergamon Press, 1964. 219
15 Elisei F et al. Nucl. Instrum. Methods A, 1997, **400**(1): 53–68
16 XIAO Hua-Lin et al. Chinese Physics C, 2010, **34**(05): 571–575
17 XIAO Hua-Lin et al. Chinese Physics C, 2010, **34**(11): 1724–1728
18 Alimonti G et al. Nucl. Instrum. Methods A, 2000, **440**(2): 360–371